Water Research 159 (2019) 223–232

Contents lists available at ScienceDirect

Water Research

journal homepage: www.elsevier.com/locate/watres

NanoSIMS reveals unusual enrichment of acetate and propionate by an anammox consortium dominated by *Jettenia asiatica*

Yu Tao [a, 1], Xiaoli Huang [a, 1], Dawen Gao [a, b, *], Xiaolong Wang [a], Chunhong Chen [a], Hong Liang [b], Mark C.M. van Loosdrecht [c]

[a] State Key Laboratory of Urban Water Resource and Environment, Harbin Institute of Technology, Harbin, 150090, China
[b] School of Environment, Harbin Institute of Technology, Harbin, 150090, China
[c] Department of Biotechnology, Delft University of Technology, Delft 2629 HZ, the Netherlands

ARTICLE INFO

Article history:
Received 17 January 2019
Received in revised form
2 May 2019
Accepted 3 May 2019
Available online 9 May 2019

Keywords:
Anaerobic ammonium oxidation
Anammox
Acetate
Propionate

ABSTRACT

Anaerobic ammonium-oxidizing (anammox) bacteria convert ammonium and nitrite into N_2 in a chemolithoautotrophic way, meaning that they utilize CO_2/HCO_3 solely as their carbon sources. Such autotrophic behavior limits their competitiveness with heterotrophic microorganisms in both natural environments and engineered systems. Recently, environmental metagenomic results have indicated the capability of anammox bacteria to metabolize short-chain fatty acids, further confirmed by limited experimental evidence based on highly enriched cultures. However, clear evidence is difficult to get because of the limits of traditional methodologies which rely on the availability of a pure anammox culture. In this study, we identified and quantified the uptake of acetate and propionate, on a single-cell level, by an anammox consortium that was dominated by *Candidatus Jettenia asiatica* (relative abundance of 96%). The consortium, growing in granular form with an average relative abundance of anammox bacteria of 96.0%, was firstly incubated in a ^{13}C-labelled acetate or propionate medium; then microtome sections were scanned by a nanometer-scale secondary ion mass spectrometer (NanoSIMS). The NanoSIMS scannings revealed that the consortium enriched acetate and propionate at a >10 times higher efficiency than bicarbonate incorporation. Our results also suggest that acetate or propionate was likely not assimilated by *J. asiatica* directly, but firstly oxidized to CO_2, which then served as carbon sources for the follow-up autotrophy in *J. asiatica* cells. Furthermore, more [^{15}N]ammonium was enriched by the propionate-fed consortium than the acetate-fed consortium despite that exactly the same amount of ^{13}C atoms were supplied. Our study strongly indicates an alternative lifestyle, namely organotrophy, in addition to chemolithoautotrophy of anammox bacteria, making it more versatile than often expected. It suggests that the niche of anammox bacteria in both natural and engineered ecosystems can be much broader than usual assumed. Recognising this is important for their role in wastewater treatment and the global nitrogen turn-over rates.

1. Introduction

Energy-efficient wastewater treatment (EEWT) processes are currently intensively studied for both environmental and economic considerations. An autotrophic anaerobic ammonium oxidation (anammox) process for nitrogen removal from municipal wastewater is known as the “mainstream anammox”, which has been confirmed to be an EEWT process in labs and holds a substantial potential in future large-scale applications. However, the mainstream anammox is challenged by several issues such as a high BOD_5/N ratio in the wastewater, competition from heterotrophic denitrifiers and nitrite oxidizing bacteria (NOB) for nitrite, strict temperature requirements, and slow growth rates of anammox bacteria.

A microorganism's mixotrophic lifestyle is a selective advantage in nature, and such capability is especially important to species that are critical to global nutrient cycles (Matin, 1978). Versatile lifestyles have been discovered in microbial cells because of the development of observation power (Hawley et al., 2014; Rother and

* Corresponding author. State Key Laboratory of Urban Water Resource and Environment, Harbin Institute of Technology, Harbin, 150090, China.
E-mail address: gaodw@hit.edu.cn (D. Gao).
[1] The authors contributed equally to this work.

https://doi.org/10.1016/j.watres.2019.05.006
0043-1354/

Metcalf, 2004), which expanded our knowledge on microbial functionality and niche.

Anaerobic ammonium-oxidizing (anammox) bacteria are capable of coupling ammonium and nitrite to form nitrogen gas under anaerobic conditions (Kuenen, 2008). They are critical players in the global nitrogen cycle (Canfield et al., 2010; Kuypers et al., 2003; Ward, 2013; Zhu et al., 2013) and have been successfully exploited to treat wastewater (Kartal et al., 2010). Most anammox species, such as *Kuenenia stuttgartiensis*, *Jettenia asiatica*, *Brocadia fulgida*, and *Scalindua profunda*, use inorganic carbon to synthesize organic molecules via a Wood-Ljungdahl pathway (also known as reductive acetyl-CoA pathway) (Gori et al., 2011; Hu et al., 2012). Rather than generating energy, this route requires high energy input, which is available from the hydrazine metabolism (Kartal et al., 2011).

As the energy release via acetate oxidation coupled to nitrite reduction is close to that of the anammox process (−359.8 kJ vs. −357.8 kJ, standard Gibbs free energy for each process calculated at pH = 7.0, temperature = 25 °C, air pressure = 101,325 Pa)(Gao and Tao, 2011), it is of interest to evaluate if anammox bacteria can convert organic matter for cell growth. Understanding of this conversion might give insight into some essential eco-technical questions, such as whether anammox bacteria can survive or have an competitive advantage in an environment where organic matter is sufficient but lacks CO_2 (Babbin et al., 2014), or is an industrial anammox process applicable in a mainstream wastewater treatment (Kartal et al., 2010)?

An organotrophic alternative has been proposed (Strous et al., 2006) and shown in laboratory settings (Kartal et al. 2007, 2008). Two organotrophic species, i.e., *Candidatus Anammoxoglobus propionicus*, *Candidatus Brocadia fulgida*, have been indicated to oxidize short-chain fatty acids into CO_2, which is then assimilated via an acetyl-CoA pathway that is predominant in the autotrophic anammox bacteria (Schouten et al., 2004). However, there have been very limited follow-up studies, and the organotrophic lifestyle of anammox bacteria is underexplored.

The discovery of an organotrophic lifestyle by anammox bacteria is often challenged by interference from heterotrophic microorganisms that co-exist in any anammox consortium. Direct observation of organotrophic processes on a single-cell level could deliver profound information about the actual physiology anammox bacteria. However, such studies are scarce by far. In recent years, nanometer-scale secondary ion mass spectrometry (NanoSIMS) has enabled to gain an in-depth view of microbiology, for example, to track microbial interactions and to study microbial metabolic activities (Kopf et al., 2015; Musat et al. 2012, 2016). In this study, we used a NanoSIMS to visualize and quantify the incorporation of ^{13}C-labelled acetate and propionate by a highly enriched anammox consortium that was dominated by *Candidatus Jettenia asiatica (Hu* et al. *2012)*. This microorganism has not yet been reported relating to organotrophy. The results that were based on 279 scans of 4885 cells strongly indicated that the anammox consortium incorporated acetate and propionate at a rate even higher than the uptake rate of bicarbonate.

In a mainstream anammox system, organic matter present in wastewater plays a key role in governing the balance between anammox bacteria and heterotrophic microorganisms such as denitrifying bacteria. Although it has been accepted that anammox bacteria are protected by heterotrophs when organic carbon is present (Li et al., 2016), our study confirms that anammox bacteria are capable of dealing with organic matters by their own. The niche of anammox bacteria in engineered ecosystems can therefore be much broader than general assumed. It also reminds us that their actual contribution to the global nitrogen turnover warrants more exploration.

2. Materials and methods

2.1. Study design

In this study, we firstly harvested relatively mature anammox granules from a 70 m^3 full-scale anammox reactor. It is located at the sludge treatment site Sluisjesdijk (Rotterdam, NL), which treats the sludge of a municipal wastewater treatment plant Dokhaven. Its actual loading was on average 700 kg-N/d following a nitritation reactor (van der Star et al., 2007). Then, we cultivated the anammox granules in a well-controlled lab-scale reactor for further enrichment of anammox bacteria. A highly enriched anammox consortium was then achieved, facilitating the next-step cultivations in different carbon sources labelled with isotopic ^{13}C.

A nanometer-scale secondary ion mass spectrometry (NanoSIMS) was used to visualize and quantify the incorporation of those isotopic element signals based on the scannings of a large number of cells in different incubations (Fig. 1).

2.2. Enrichment of J. asiatica

An expanded granular sludge bed (EGSB) is a typical high-efficiency bioreactor used for wastewater treatment under anaerobic conditions (Connelly et al., 2017). The 1.2 L EGSB was inoculated with anammox aggregates that were obtained from a full-scale anammox bioreactor that treated centrifuged sludge digestate. The influent flow rate was 13.2 L/d, which corresponded to hydraulic retention time (HRT) of 1.82 h. An up-flow velocity of 4.8 m/h was maintained by bulk circulation in order to keep granulation. The temperature was controlled at 34 ± 1 °C using a heating jacket. The medium was sparged with a gas mixture of N_2 and CO_2 (95% and 5%, respectively) for 20 min after each time of preparation in order to remove oxygen. The primary sources of the medium were $(NH_4)_2SO_4$ (5–14 mM) and $NaNO_2$ (5–17.5 mM). The medium also contained the following compounds (per 1 L demineralized water): $KHCO_3$ (1000 mg), KH_2PO_4 (27.2 mg), $MgSO_4 \cdot 7H_2O$ (240 mg), $CaCl_2$ (300 mg), and trace element solution I and II (1 mL, respectively, prepared according to (van de Graaf et al., 1996)). The pH of the fresh medium was 7.6 ± 0.3 without neutralization. The feeding for the EGSB was shut down for 48 h before collecting consortium samples, allowing the removal of the residual ammonium, nitrite, and bicarbonate in bulk.

2.3. Medium

The isotope medium contained ^{13}C- and ^{15}N-labelled chemicals that were supplied by Cambridge Isotope Laboratories (Tewksbury, MA, USA). The oxygen-free medium was prepared using ultra-pure water and sparged with N_2 gas (99.99% purity) for 30 min in an anaerobic glove box. Resazurin was used as an anaerobic indicator in the medium.

Eight groups of experiments were carried out with seven (Group 1–7) applying 2.0 mM [^{15}N]ammonium and 2.0 mM [^{14}N]nitrite as nitrogen sources, and one (Group 8) using 2.0 mM [^{15}N]nitrate only (Table 1). For each incubation, a total of 2.5 μmol ^{13}C atoms were supplied no matter in bicarbonate, acetate or propionate forms. Group 1 mimicked a typical anammox process with [^{13}C]bicarbonate as the sole carbon source. The Group 2–5 applied acetate-centred carbon sources, including [1–^{13}C]acetate (Group 2), [2–^{13}C]acetate (Group 3), [^{13}C]bicarbonate+[^{12}C]acetate (Group 4), and [^{13}C]bicarbonate+[2–^{13}C]acetate (Group 5). Group 6 and 7 applied propionate-centred carbon sources, including [1–^{13}C]propionate (Group 6), [^{13}C]bicarbonate+[^{12}C]propionate (Group 7). [2–^{13}C]acetate was used in Group 8 in order to check the contribution of heterotrophic bacteria (e.g., denitrifying bacteria) in the consortium.

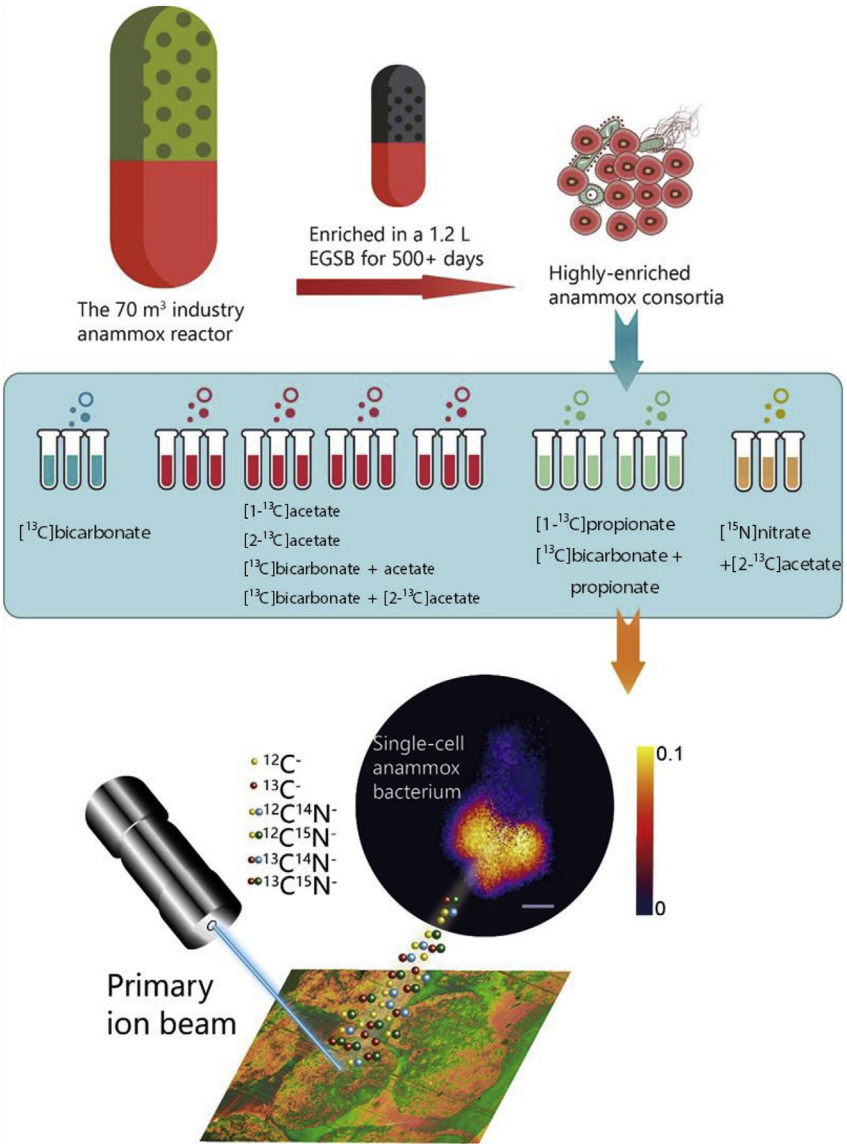

Fig. 1. Experimental design and schematic of single-cell tracking of anammox bacteria. The original biomass was collected from a full-scale anammox reactor, and then they were enriched in a lab-scale reactor using a classic anammox-bacteria culturing medium. The highly enriched anammox bacteria were firstly confirmed by fluorescence *in situ* hybridization (FISH) and then incubated in the medium that contained isotopic substrates, i.e., ^{15}N-labelled ammonium, nitrite, and ^{13}C-labelled carbon sources (bicarbonate and/or acetate, propionate). The incubation was carried out for both short-term (five, ten, twenty, and 60 min) and long-term (twenty, 24 h, and fifteen days). A NanoSIMS was used to determine the incorporation of ^{13}C and ^{15}N in the cells. A primary Cs^+ beam generates negative secondary ions from the cell zones of a specimen. Substantial incorporation of ^{15}N was then confirmed by the high signal of $^{12}C^{15}N^-$ mass (yellow color in the core of the cell). Other masses such as $^{12}C^-$, $^{13}C^-$, $^{12}C^{14}N^-$, $^{31}P^-$ and $^{56}Fe^{16}O^-$ were also recorded simultaneously. (For interpretation of the references to color in this figure legend, the reader is referred to the Web version of this article.)

2.4. Incubation

For each incubation, 4–5 anammox granules were randomly selected to incubate in a 12 mL Hungate tube. A volume of 5 mL media was added to each tube. Triplicate incubations were done for each group and gently shaken at 30 °C in the dark anaerobically. The incubations were ended by dosing 200 μl of 8 M $ZnCl_2$ solution after 30 s, 5 min, 10 min, 20 min, 1 h, 20 h, and 15 d, respectively. The reason for applying frequent sampling within the first hour is to avoid missing the endings of reactions, especially the rapid

Table 1
The eight groups of isotope media used in this study.

Group	Nitrogen sources	Inorganic carbon sources	Organic carbon sources
1	[^{15}N]ammonium+[^{14}N]nitrite	[^{13}C]bicarbonate	none
2	[^{15}N]ammonium+[^{14}N]nitrite	none	[1–^{13}C]acetate
3	[^{15}N]ammonium+[^{14}N]nitrite	none	[2–^{13}C]acetate
4	[^{15}N]ammonium+[^{14}N]nitrite	[^{13}C]bicarbonate	[^{12}C]acetate
5	[^{15}N]ammonium+[^{14}N]nitrite	[^{13}C]bicarbonate	[2–^{13}C]acetate
6	[^{15}N]ammonium+[^{14}N]nitrite	none	[1–^{13}C]propionate
7	[^{15}N]ammonium+[^{14}N]nitrite	[^{13}C]bicarbonate	[^{12}C]propionate
8	[^{15}N]nitrate	none	[2–^{13}C]acetate

nitrogen conversions. The 20 h and 15 d incubations were also carried out in order to allow a complete cell cycle as the doubling time of anammox bacteria can be as long as 1–2 weeks (Jetten et al., 1998; van Niftrik and Jetten, 2012). For the 15-day incubations, 0.5 mL supernatants of the original medium were replaced for every three days by the concentrated medium that contained 20 mM $^{15}NH_4Cl$ and $Na^{14}NO_2$, respectively, while no such replacement of medium being done to the other incubations.

2.5. DNA extraction

The anammox granules samples were taken from EGSB reactors and stored at −80 °C until the DNA extraction. The granules were washed with 1 × phosphate buffer saline (PBS) solution and then centrifuged at 7000 × G for 7 min. The supernatant was removed, and the pellet was washed with the same PBS solution for the second time and centrifuged under 17,000 × G for 20 min. The supernatant was removed, and the pellet was used for the DNA extraction. The DNA isolation was performed using a UNIQ-10 DNA Isolation Kit (Sangon Biotech Co., Ltd, Shanghai, China) as per the manufacturer's instructions. The DNA isolation was confirmed by an agarose gel electrophoresis. The quality of DNA was verified by a Nanodrop 1000 equipment (Thermo Scientific, Waltham, MA, USA).

2.6. qPCR

The number of anammox bacteria was tested by an SYBR-Green qPCR method. The reaction mixture contained 10 μl of 2 × SGExcel Fast SYBR Mixture (with ROX, Shanghai Sangon Biological Engineering Technology & Services Co., Ltd. China), 3 μl of the template DNAs, 1 μl of forward and reverse primers. The qPCR for universal bacteria was done on the hypervariable V3 region of the 16S rRNA gene, i.e., the primer pair for universal eubacterial 16S 338f (5′–ACTCCTACGGGAGGCAGCAG–3′) and 518r (5′–ATTACCGCGGCTGCTGG–3′) (Harshman et al., 2015). The primer sets for anammox bacteria were hzocl1F1 (5′–TGYAAGACYTGYCAYTGG–3′) and hzocl1R2 (5′–ACTCCAGATRTGCTGACC–3′) (Schmid et al., 2008). The qPCR was performed using an ABI7500 instrument (Foster City, CA, USA). The program assay consisted of 30 min of denaturation at 95 °C, 40 cycles of 30 s at 95 °C, 30 s at 94 °C, annealing (1 min at 55 °C) and elongation (1 min at 72 °C). The real-time detection was performed at the annealing stage. A melt curve analysis was performed for confirming the binding specificity of a primer pair. Each sample was run in triplicate wells. The plasmid DNA (Beijing Microread Gene Technology Co., Ltd.) was diluted seven times, yielding a series of final concentration from 1.9×10^1 copies/mL to 1.9×10^9 copies/mL and a standard curve was established with an average slope of −3.302. The threshold cycle (C_T) values were plotted against the logarithm of their initial copy concentrations. All the standard plasmids and the DNA samples were amplified in triplicate.

2.7. Fluorescence in situ hybridization (FISH)

A FISH analysis was performed to quantify the percentage of anammox bacteria according to the protocol described by Schmid et al. (2005). In brief, the anammox samples were firstly mixed with 4% paraformaldehyde for fixation and then placed onto a gelatin-coated slide. After the dehydration, the cells were hybridized with the fluorescently labelled oligonucleotide probe S-*-Amx-0368-a-A-18r (5′–CCTTTCGGGCATTGCGAA–3′) (Sangon Biotech Co., Ltd, Shanghai, China) and counterstained using a 4, 6-diamidino-2-phenylindole (DAPI) (Sangon Biotech Co., Ltd, Shanghai, China). The microscopic observations were performed using an Olympus fluorescence microscope (BX2U-MWU2, Olympus, Japan).

2.8. Transmission electron microscopy (TEM)

The TEM was carried out to observe the anammox cell morphology in the EGSB granules. The biomass samples taken from the EGSB were fixed with 2.5% glutaraldehyde in 0.1 mM sodium phosphate buffer (pH 7.2) under 4 °C. Then the granules were dehydrated through a gradient ethanol series (75%–100%) and 100% acetone. After that, the samples were embedded with ethoxyline 618 and sliced into 60-nm specimens by a microtome (LKB-V, LKB, Sweden). Finally, the thin slices on the copper net were double stained with uranyl acetate and lead citrate and then observed by a TEM instrument (JEM100-SX, JEOL, Japan).

2.9. Preparation of the specimens for NanoSIMS analysis

The biomass samples were firstly fixed with 2.5% glutaraldehyde, rinsed in phosphate-buffered saline (PBS), and then dehydrated in a graded series of ethanol solution (50%, 70%, 90%, and 100%) and an ethanol-acetone mixture solution at 4 °C, subjected to two 20-min changes of dry acetone to remove water. Three infiltration steps (3 h for each) were carried out using (1) 2 acetone: 1 EMbed 812-Araldite resin mixtures; (2) 1 acetone: 2 EMbed 812-Araldite resin mixtures and; (3) pure EMbed 812-Araldite. The polymerization was done in capsules for 24 h at 60 °C. The ultrathin sections (60–70 nm, for TEM tests) were sliced from the resin blocks using an Ultramicrotome (LKB-V, LKB, Sweden) and mounted on copper grids, then stained with saturated alcoholic uranyl acetate and lead citrate. The sections were examined by a Jeol JEM100SX electron microscope (Tokyo, Japan). The thin sections (600 nm, for NanoSIMS) were sliced from the remained resin blocks with glass knives and then mounted on the pre-coated quartz wafer disks, followed by a coating with 10-nm gold.

2.10. NanoSIMS analysis

The incorporation of nitrogen and carbon isotopes was determined using a CAMECA NanoSIMS 50 L instrument at the Beijing SIMS Lab, Chinese Academy of Sciences. The Cs^+ primary beam was used with an accelerating high voltage of 8 kV. A mass resolution power of ~7000 (M/M, 10% definition) was applied, enough to eliminate isobaric interference of $^{13}C^-$ by $^{12}C^1H^-$, and $^{12}C^{15}N^-$ by $^{12}C^{14}N^1H^-$. Samples were pre-sputtered with a primary Cs^+ beam of ~1 nA for 2 min, in order to remove the gold coat and achieve stable yield rates of the secondary ions. After pre-sputtering, secondary ion images of $^{12}C^-$, $^{13}C^-$, $^{12}C^{14}N^-$ (for ^{14}N), $^{12}C^{15}N^-$ (for ^{15}N), $^{31}P^-$ and $^{56}Fe^{16}O^-$ (for Fe) ions were acquired with electron multipliers (EMs) in a multi-collection mode, rastering a ~1 pA Cs^+ primary beam (~100 nm in diameter) over an area of 20 μm × 20 μm (Fig. S1) of the samples (3 μm × 3 μm for some high-resolution rastering). Each frame of the images consists of 256 pixels by 256 pixels, and the dwell time was 10 ms/pixel. Three layers were corrected for image shift and then accumulated into a single image. Two randomly selected areas of each sample were analyzed to ensure proper surface electric conduction.

2.11. NanoSIMS image processing

All the NanoSIMS scans were analyzed using the software OpenMIMS, an open-source ImageJ plugin that is supported by the National Resource for Imaging Mass Spectrometry (http://www.nrims.hms.harvard.edu/). All the analysis was done under PC Windows environment. The quantification of ^{15}N and ^{13}C

incorporation were determined by selecting those regions of interest (ROIs) that were defined manually, following three strict criteria: (1) the sizes of the targeted cells were in the range of 800–1200 nm; (2) the cells were coccoid or coccoid-like shape (van Niftrik and Jetten, 2012) and; (3) the $^{15}N/^{14}N$ hotspots can well wedge into the web-like distributions of ^{31}P precipitants, which are highly expected to be excreted by anammox bacteria.

For $\delta^{13}C$ and $\delta^{15}N$ data processing, the $^{15}N/^{14}N$ and $^{13}C/^{12}C$ values of the anammox granules that were cultivated for 30 s were used as the standard for calculation and calibration. The δ value was calculated as $\delta=(R_{sample}/R_{standard})-1$, where R_{sample} stands for isotopic ratios of $^{13}C/^{12}C$ and $^{15}N/^{14}N$, and $R_{standard}$ is the $^{13}C/^{12}C$ and $^{15}N/^{14}N$ values of the samples after 30s incubation.

3. Results

3.1. The enrichment of J. asiatica in the cultivation bioreactor

The enrichment of *J. asiatica* was carried out in an expanded granular sludge bed (EGSB) reactor that was fed with a standard medium for cultivating anammox bacteria (Fig. 1). No organic matter was added to the EGSB. Red-colored granule-like aggregates were formed in the EGSB, and the size of granules increased to and stabilized at 1–2 mm during the cultivation (Fig. 2a). Some granules contained interstitial voids (Fig. S1) that might serve as water or gas channels, benefitting to mass transportation (Lu et al., 2012). Fluorescence *in situ* hybridization (FISH) analysis confirmed that the microbial consortium was dominated by anammox bacteria with a mean relative abundance of 96.0% (Fig. 2b), identified as *J. asiatica* by 16S rRNA sequencing (GenBank: KJ002641.1). A classic anammox cell architecture and compartmentalization were confirmed by transmission electron microscopy (TEM) (Fig. 2c), clearly showing anammoxosome as the central organelle (van Niftrik et al., 2008).

The ammonium-oxidation capacity of the EGSB increased by approximately ten times after a long-term operation (Figs. 1 and 2d). Meanwhile, the qPCR analysis showed that the *hzo* gene copy numbers of the EGSB biomass increased by over five orders of magnitude (Fig. 2d). The *hzo* gene encodes for the enzyme hydrazine oxidoreductase converting hydrazine to N_2 (Li et al., 2011; Pitcher et al., 2011), which is a unique metabolic process specific for anammox bacteria (Kartal et al., 2011). The ratio of the consumed nitrite to the consumed ammonium stabilized in the range of 1.30–1.37, while the ratio of the produced nitrate to the consumed ammonium was consistently in the range of 0.20–0.25, both of which agreed with known anammox stoichiometry (Walter et al., 1999).

3.2. Classic anammox reaction

Intense incorporation of ^{15}N (coming from [^{15}N]ammonium) by the consortium was identified by nanoSIMS after only 10 min of incubation but soon decreased in the control group that mimics a typical anammox reaction (Group 1, Fig. 3b). The weak signal of ^{15}N was very likely due to the formation of $^{15}N_2$ which escaped from the cytoplasm easily. This result strongly indicated that ammonium oxidation was very efficient in the consortium, taking place even within several minutes.

The short-term incubations (5–60 min) of Group 1 exhibited minimal enrichment of ^{13}C, while a 2–4 times higher uptake of ^{13}C was observed in the 20-h and 15-day incubations (Fig. 3a). According to our NanoSIMS analysis of the 20-h incubation, the ratio of $\delta^{13}C/\delta^{15}N$ was 21/1000, which was similar to a previous report that showed a stoichiometry of 20 mmol CO_2 incorporations per mol ammonium consumption (Strous et al., 1999).

For Group 8 that mimicked a typical denitrification reaction

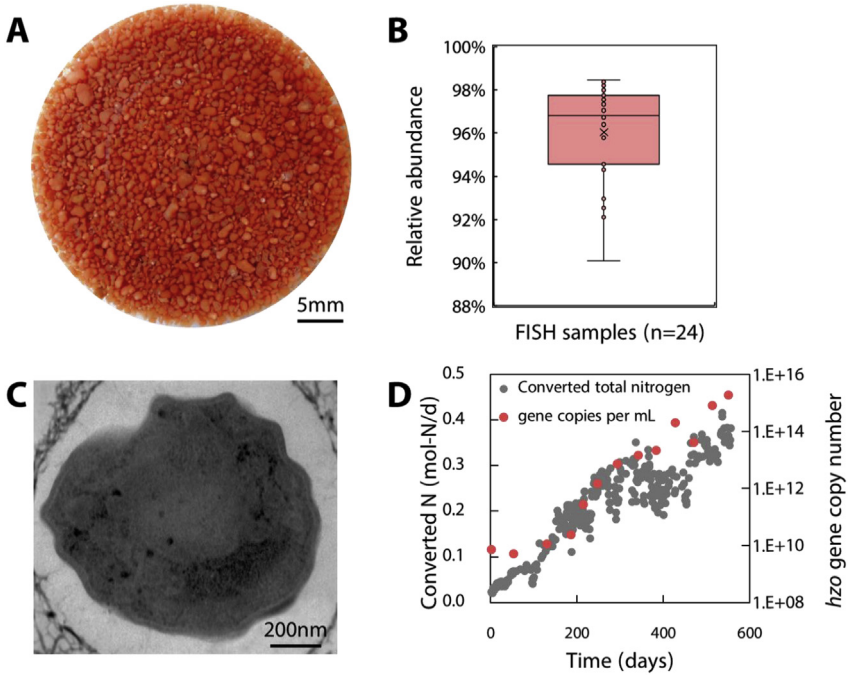

Fig. 2. Enrichment and confirmation of anammox bacteria. (A) A photo of the enriched red-color anammox granules, which is a typical color of anammox consortia/granules. Most of the granules have the diameters of 1–2 mm. (B) shows the relative abundance of anammox bacteria in the community calculated based on the FISH images of twenty-four different samples. (C) shows a transmission electron microscopy (TEM) image of an anammox bacterium in the anammox granule. A large compartment as anammoxosome can be observed. (D) The changes of the total converted nitrogen and the number of anammox bacteria during the 500-day enrichment. The anammox bacteria quantity was shown as the *hzo* gene copy numbers, which represents a functional gene of anammox bacteria. (For interpretation of the references to color in this figure legend, the reader is referred to the Web version of this article.)

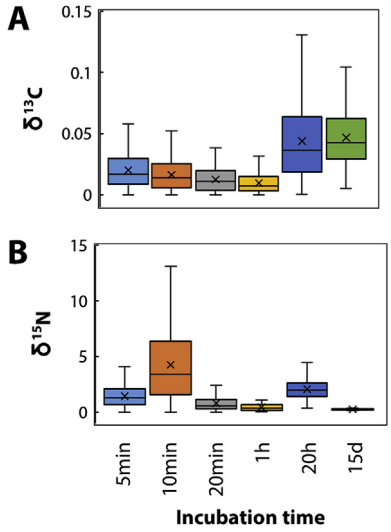

Fig. 3. $\delta^{13}C$ and $\delta^{15}N$ of the control group after the incubation of a wide range of time from 5 min to 15 days.

with [^{15}N]nitrate as electron acceptor and [2−^{13}C]acetate as electron donors (Table 1), we confirmed the presence of >100 cells, which was suggested from the observation of matrix rings according to the ^{31}P NanoSIMS scans, which indicated the existence of lipid bilayers (Fig. S2c). However, we could observe only two ^{15}N signals (Fig. S2b) and extremely weak incorporation of [2−^{13}C]acetate (Fig. S3). Since strong incorporation of [2−^{13}C]acetate would occur if heterotrophic microorganisms were abundant in the consortium, our findings of very low incorporation of [2−^{13}C]acetate suggested that a very low fraction of heterotrophs (e.g., denitrifying bacteria) could be present.

3.3. Acetate- and propionate-engaged anammox processes

The cells in the [2−^{13}C]acetate-added (Group 3) and the [1−^{13}C]propionate-added (Group 6) groups enriched acetate and propionate, respectively according to the NanoSIMS scans (Fig. 4). Furthermore, the ^{13}C signals distributed across a large area of individual cells rather than a particular location (Figs. 4a and 5a). The NanoSIMS images of a single cell (Fig. 5 and Fig. S4), dividing cells (Fig. S5 and Fig. S6) and multiple cells (Fig. S7 and Fig. S8) consistently suggested that the highly enriched ^{13}C region well matched to the ^{15}N hot zones (Pearson correlation values range 0.853−0.947) (Figs. 4a, 5a and g, 5h), which likely were anammoxosome (Dietl et al., 2015).

Higher enrichment of ^{15}N and ^{13}C can be seen in the 15-day incubations compared to short ones (Fig. 6). For the 15-day incubations, the propionate-fed consortium incorporated more ^{13}C than the acetate-fed one, and all the organic carbon groups (Group 2−7) enriched more ^{13}C than the control group (Group 1) (Fig. 6). For the 20-min and 1-h incubations, the ^{13}C incorporation was not significantly different among each group except for Group 6, which was fed with [1−^{13}C]propionate. The ^{15}N incorporation of each incubation was also in a similar level, except for the [1−^{13}C]acetate-added group (Group 2), which was significantly higher than the others.

The addition of unlabelled acetate (Group 4) or propionate (Group 7) boosted the incorporation of ^{13}C by 70 and 27 times compared to the incorporation in the control group (Group 1) after 15-d incubation (Fig. 6). The time courses of the acetate- and propionate-aid [^{13}C]bicarbonate assimilation showed that the incorporation was not significant within 20 h, but was evident on day 15 (Fig. S9a and S9c). The nitrogen incorporation also had

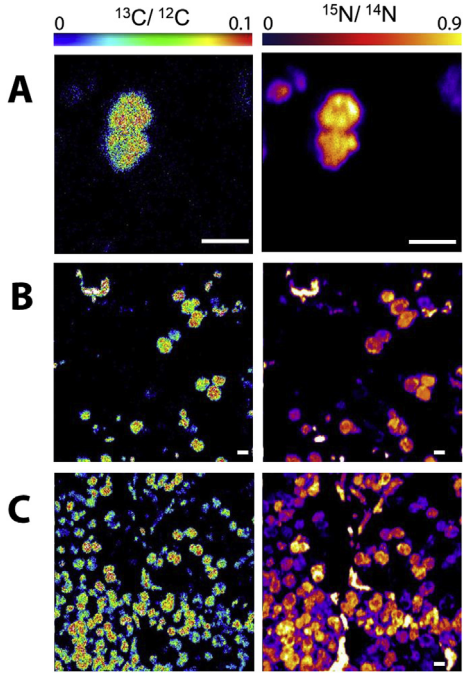

Fig. 4. NanoSIMS images showing the incorporation of acetate and propionate. (A), the images of the ^{13}C/^{12}C and ^{15}N/^{14}N distribution in a dividing anammox cell after 15-day cultivation in [2−^{13}C]acetate. The hot color represents the high enrichment of ^{13}C and ^{15}N in the cells, respectively. The two cells are unlikely two individual cells because the incorporated ^{15}N was evenly dispersive along the border. (B), the ^{13}C/^{12}C and ^{15}N/^{14}N distribution in a community that had 81 recognizable cells after 15-day cultivation in [2−^{13}C]acetate. (C), the ^{13}C/^{12}C and ^{15}N/^{14}N distribution in a community with 170 recognizable cells after 15-day cultivation in [1−^{13}C]propionate. The scale bars represent 1 mm for all the images. (For interpretation of the references to color in this figure legend, the reader is referred to the Web version of this article.)

similar trends (Fig. S9b and S9d). It was a strange phenomenon and might be linked to unknown pathways of *J. asiatica* in the presence of acetate or propionate.

4. Discussion

4.1. Is there a heterotrophic anammox conversion?

Heterotrophs are those organisms that require organic substrates as a carbon source for growth (Claassens et al., 2016). In our study, *J. asiatica* was proven to be able to take-up acetate and propionate. A core question followed will be obvious. Did they utilize those short-chain fatty acids for forming biomass of their own (for growth)?

If *J. asiatica* carried out a heterotrophic anammox process, the ^{13}C labeling position on the methyl (Group 2, [1−^{13}C]acetate-added group) or carboxyl (Group 3, [2−^{13}C]acetate-added group) carbon of acetate would result in no differences in terms of the eventual ^{13}C incorporation. However, we found significantly higher ^{13}C enrichment in the [2−^{13}C]acetate-added group (Group 3) than that in the [1−^{13}C]acetate-added group (Group 2) after 15 days (Fig. 6). It indicated that the acetate or propionate was likely not assimilated by *J. asiatica* directly, but oxidized to CO_2, which then served as carbon sources for the follow-up autotrophic growth of *J. asiatica*.

It still warrants more experimental work to confirm a metabolic pathway behind the organic carbon utilization by *J. asiatica* as we are still not able to completely rule out the possibility of *J. asiatica* assimilating acetate or propionate. From another perspective, some genomic and proteomic discoveries indicate that some anammox bacteria might directly incorporate acetate into their cell biomass. For example, carbon monoxide (CO) dehydrogenase/acetyl-CoA

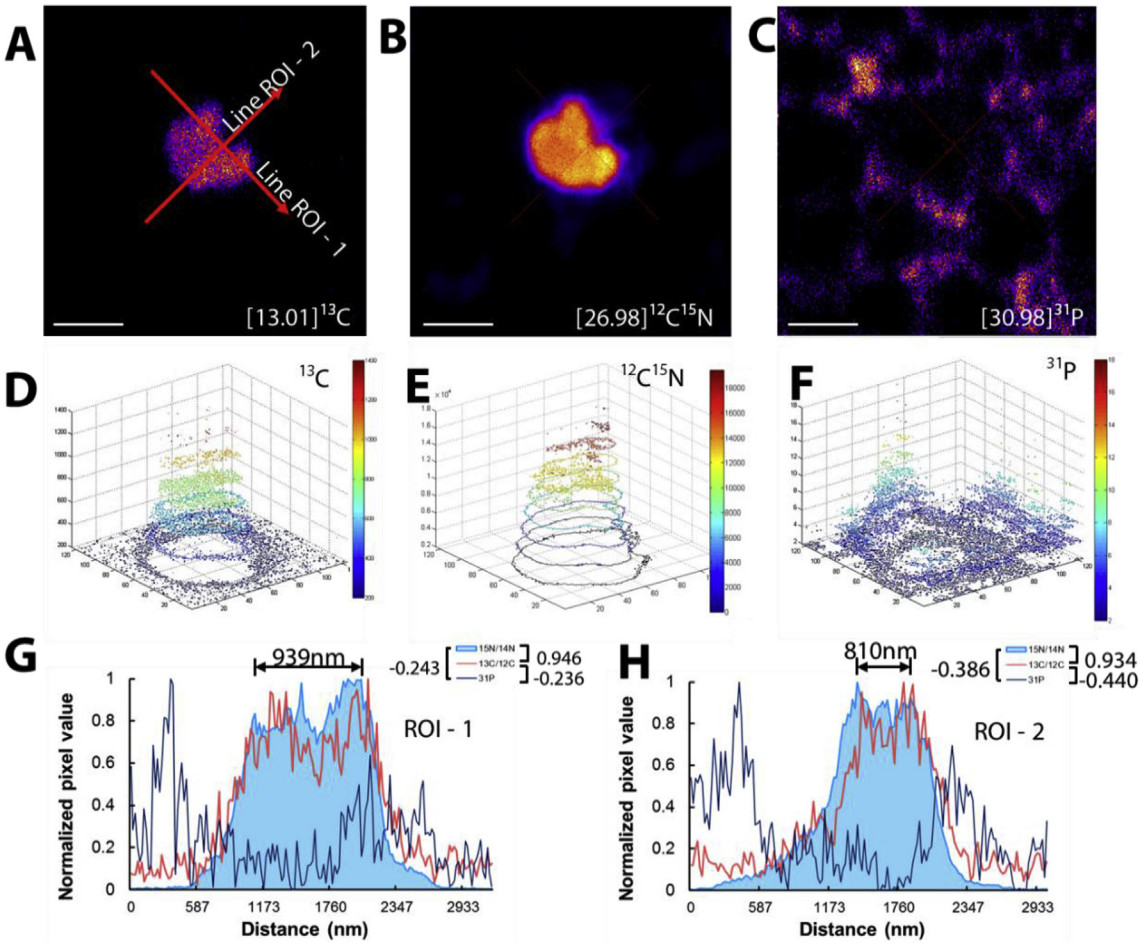

Fig. 5. Simultaneous enrichment of ^{13}C, ^{15}N, and ^{31}P by a single cell of anammox bacteria cultivated with [^{13}C]bicarbonate and propionate after fifteen days. (A), (B), and (C), NanoSIMS images showing a single cell enriching ^{13}C, ^{15}N and ^{31}P, respectively. Scale bar: 1 μm. (D), (E), and (F), the distribution of high ^{13}C, ^{15}N and ^{31}P content within the anammox bacteria cell. The values show the signal strength of ^{13}C, $^{12}C^{15}N$ and ^{31}P ions by NanoSIMS. The hot colors illustrate high enrichment while the cold colors indicate little enrichment. (G) and (H) show the enrichment of ^{13}C, ^{15}N, and ^{31}P along two linear regions of interest (ROI). The values are normalized in order to compare the pairing trend of each ion easily. It is evident to see that the ^{13}C and $^{12}C^{15}N$ ions share very similar dynamics in both line ROIs, while the ^{31}P ions have an opposite trend of dynamics. The high ^{13}C and $^{12}C^{15}N$ enrichment zones range from 800 to 1000 nm in the distance. The values of Pearson correlation are listed on the top right of figures (G) and (H). (For interpretation of the references to color in this figure legend, the reader is referred to the Web version of this article.)

synthase (*acs*) is responsible for the CO_2 fixation, and it is shared by many anammox species such as *K. stuttgartiensis, S. profunda*, *J. caeni*, and *J. Asiatica* (Muhammad et al., 2015; Oshiki et al., 2016). The transcriptome and proteome of *K. stuttgartiensis*, the model species of anammox bacteria, show high-level genes encoding of pyruvate-associated enzymes such as pyruvate oxidoreductase (kuste4371) and pyruvate carboxylase (kustd1409) (Kartal et al., 2011). The metagenome of the marine anammox bacterium *S. profunda* illustrates several genes encoding acetate kinase, phosphotransacetylase, pyruvate kinase, and pyruvate ferredoxin oxidoreductase, indicating a versatile carbon metabolism *in situ* (van de Vossenberg et al., 2013). It has been found that acetate can be activated by an acetyl-CoA synthetase-like protein (kustc1128) in a heterologous host, as well as whole cells of *K. stuttgartiensis* (Russ et al., 2012). Such acetate activation might lead to the direct incorporation of acetate into cell biomass by anammox bacteria.

4.2. Different impacts of propionate and acetate on ammonium oxidation

Carbon is important to ammonium oxidation by *J. asiatica* as a linear relationship can be found between the incorporation of ^{13}C and ^{15}N (Fig. 7) if all the cells are considered (cultivated in whatever media). Furthermore, we found different impact of propionate and acetate on the incorporation of ^{15}N. In our study, exactly the same amount of ^{13}C atoms were supplied to all anammox cells, but they tended to incorporate more [^{13}C]propionate than [^{13}C]acetate and, accordingly, more [^{15}N]ammonium was enriched by the propionate-fed consortium than the acetate-fed one (Fig. 6). It has been reported that the specific rate of acetate oxidation is higher in *B. fulgida*, while *A. propionicus* utilizes propionate faster (Jetten et al., 2009).

According to the molecular mechanism of ammonium and nitrite metabolism by anammox bacterium *K. stuttgartiensis* (Kartal et al., 2011), the generation of NO and N_2H_4 requires a significant amount of electron equivalents (Eq. (1) and (2)). When acetate or propionate was oxidized to CO_2 firstly, such oxidation would offer a large number of electrons. For example, the oxidation of acetate yields 8 electron equivalents while propionate yields 14. Considering the very close relationship between ^{13}C and ^{15}N incorporation, it is possible that these electrons are used to produce NO and N_2H_4. As a compelling electron donor ideal for the reduction of CO_2 (the oxidized product of acetate or propionate), N_2H_4 supplied the reductive acetyl-CoA pathway with adequate electrons from the oxidation of N_2H_4 to N_2 that yields 4 electrons (Eq. (3)).

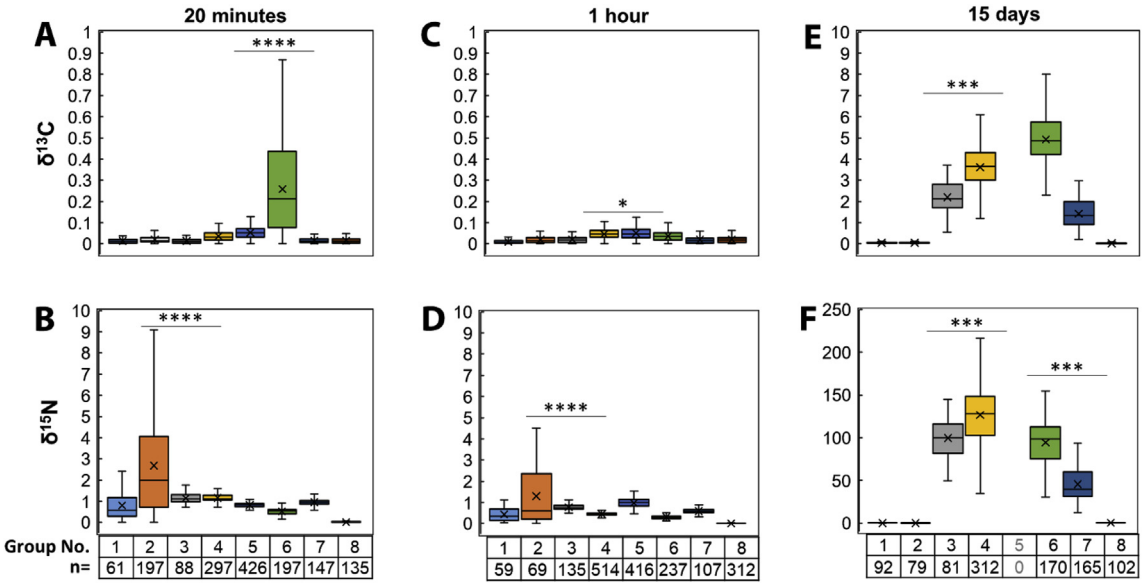

Fig. 6. The quantification of the incorporated ^{13}C-labelled bicarbonate, acetate, and propionate at 20 min, 1 h, and 15 d. The cell number of each group that was accounted in the interpretation of the NanoSIMS scans were also listed below the group no. of each. All the data are shown in the box and whisker charts, which illustrate the distribution of data into quartiles, highlighting the mean and outliers. The whiskers lines indicate variability outside the upper and lower quartiles, and any point outside those lines or whiskers is considered an outlier in the plots. The statistics among groups were compared by two-tailed unpaired Student's t-test, $^{*}P < 0.05$, $^{***}P < 0.001$, $^{****}P < 0.0001$.

$$NO_2^- + 2H^+ + e^- = NO + H_2O\ (E_0' = +0.38\ V) \quad (1)$$

$$NO + NH_4^+ + 2H^+ + 3e^- = N_2H_4 + H_2O\ (E_0' = +0.06\ V) \quad (2)$$

$$N_2H_4 = N_2 + 4H^+ + 4e^-\ (E_0' = -0.75\ V) \quad (3)$$

4.3. Inspirations for future studies and applications

NanoSIMS is a powerful tool to study element enrichment in cells on a single-cell level (Gao et al., 2016). In our study, the enrichment of ^{15}N and ^{13}C in *J. asiatica* was intensively monitored by NanoSIMS, beside of that, ^{31}P and ^{56}Fe enrichment was also captured, giving extra information, e.g., on the composition of the EPS matrix in anammox granules.

We found that the enrichment of ^{31}P did not correlate to that of ^{13}C and ^{15}N, but surprisingly, highly correlated to ^{56}Fe enrichment (Fig. S5 and S7). Because most highly enriched ^{31}P and ^{56}Fe zones are extracellular, it is very likely that a substantial number of extracellular polymeric substance (EPS) was formed with phosphate and iron enclosed (Cao et al., 2011; d'Abzac et al., 2013), which facilitated the forming of granules (Hou et al., 2015). There also might be iron-phosphate precipatation under suitable physiochemical conditions (Lin et al., 2013). The signal strength indicating ^{31}P and ^{56}Fe enrichment did not vary significantly along with incubation time but correlated with space strongly.

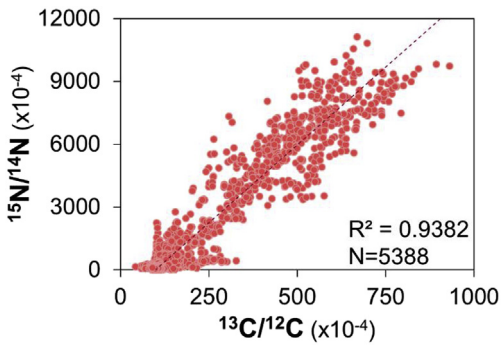

Fig. 7. The simultaneous incorporation of ^{15}N and ^{13}C by anammox bacteria cells. It is plotted based on in total 5388 times of NanoSIMS scannings over the anammox bacteria cells that were cultivated in all the groups.

It is also expected that the study could benefit our understanding of an overall contribution of anammox bacteria in a mainstream anammox process. First of all, our results showed extremely efficient incorporation of ammonium by *J. asiatica*, taking place within 5 min and reaching to maximum in 10 min (Fig. 3b). Such capability could enable *J. asiatica* to be competitive against other ammonium-dependent microorganisms. Secondly, long-term cultivation with acetate/propionate may accelerate biomass formation of *J. asiatica* cells as higher enrichment of ^{13}C was observed after 15 days (Fig. 6e), which may help *J. asiatica* sustain a dominant power in a community. Last and most importantly, anammox bacteria might be less vulnerable than previously suggested in a mainstream environment.

The organic matter is inevitable in a mainstream anammox process, and it is one of the critical factors balancing two microbial guilds, i.e., anammox bacteria and denitrifying bacteria. There have been some studies showing that (1) anammox bacteria are not vulnerable in the presence of low-dose organic matters likely because of the protection by aerobic/anaerobic heterotrophs, and (2) anammox bacteria are unlikely to grow on organic matters in a mainstream anammox process. For example, It has been found that a higher ratio of BOD_5/TN in the influent of a mainstream anammox reactor resulted in higher nitrogen-removing efficiency, very likely due to the enhanced conventional denitrification (Cao et al., 2016). It is also confirmed the growth of anammox bacteria in a mainstream anammox process, and the anammox bacteria did not directly incorporate or store the radioactive labelled acetate or glucose in their studies (Laureni et al., 2015).

Although our study confirmed the capability of anammox bacteria *J. asiatica* incorporating acetate and propionate, we do not clearly understand how they might compete with aerobic and/or denitrification heterotrophs in a mainstream anammox

environment. It definitely requires further experimental studies to explain the following questions. (1) Is such organotrophic capability only specific to *J. asiatica*, or is it a versatility to all anammox species? (2) Will short-chain fatty acids other than acetate and propionate also be incorporated under similar conditions? (3) What are the evolutionary, physiological and ecological reasons behind a detour metabolism of *J. asiatica*'s organotrophic lifestyle? (4) Is it feasible engineer truely heterotrophic anammox bacteria through the introduction of production pathways and the modification of autotrophic systems by genetic engineering?

5. Conclusions

NanoSIMS analysis of an inorganic/organic incubated, highly-enriched anammox granular consortium, reveals efficient incorporation of acetate and propionate. Although it is still an enigma how acetate and propionate are metabolized and how energy/electrons flow in the cell, the results offer essential insight to the versatility of anammox bacteria. Here, the shown organotrophic, but unlikely a heterotrophic, lifestyle of anammox bacteria strongly supports a promising niche of anammox bacteria in a mainstream anammox process where organic matter is present. Follow-up studies about how such versatility could enhance the growth of anammox bacteria are needed.

Declaration of interests

The authors declare that they have no known competing financial interests or personal relationships that could have appeared to influence the work reported in this paper.

Funding

This work was supported by the National Natural Science Foundation of China (No. 31870471, 31470543).

Conflicts of interest

The authors declare no conflict of interest.

Acknowledgments

General: We thank Prof. J. Gijs Kuenen from the Delft University of Technology for the valuable suggestions about the experimental design. We appreciate Prof. Zhonghe Pang and Prof. Yangting Lin from the Chinese Academy of Sciences for the kind advice on applying NanoSIMS analysis. The authors would also like to thank Dr. Lei Nie from the Data Science Institute, Imperial College London, for guiding the image data processing and analysis.

Appendix A. Supplementary data

Supplementary data to this article can be found online at https://doi.org/10.1016/j.watres.2019.05.006.

References

Babbin, A.R., Keil, R.G., Devol, A.H., Ward, B.B., 2014. Organic matter stoichiometry, flux, and oxygen control nitrogen loss in the ocean. Science 344 (6182), 406–408.

Canfield, D.E., Stewart, F.J., Thamdrup, B., De Brabandere, L., Dalsgaard, T., Delong, E.F., Revsbech, N.P., Ulloa, O., 2010. A cryptic sulfur cycle in oxygen-minimum-zone waters off the Chilean coast. Science 330 (6009), 1375–1378.

Cao, Y., Hong, K.B., van Loosdrecht, M.C.M., Daigger, G.T., Yi, P.H., Wah, Y.L., Chye, C.S., Ghani, Y.A., 2016. Mainstream partial nitritation and anammox in a 200,000 m(3)/day activated sludge process in Singapore: scale-down by using laboratory fed-batch reactor. Water Sci. Technol. 74 (1), 48–56.

Cao, Y.Y., Wei, X., Cai, P., Huang, Q.Y., Rong, X.M., Liang, W., 2011. Preferential adsorption of extracellular polymeric substances from bacteria on clay minerals and iron oxide. Colloids Surfaces B Biointerfaces 83 (1), 122–127.

Claassens, N.J., Sousa, D.Z., Dos Santos, V.A., de Vos, W.M., van der Oost, J., 2016. Harnessing the power of microbial autotrophy. Nat. Rev. Microbiol. 14 (11), 692–706.

Connelly, S., Shin, S.G., Dillon, R.J., Ijaz, U.Z., Quince, C., Sloan, W.T., Collins, G., 2017. Bioreactor scalability: laboratory-scale bioreactor design influences performance, ecology, and community physiology in expanded granular sludge bed bioreactors. Front. Microbiol. 8, 664.

d'Abzac, P., Bordas, F., Joussein, E., van Hullebusch, E.D., Lens, P.N.L., Guibaud, G., 2013. Metal binding properties of extracellular polymeric substances extracted from anaerobic granular sludges. Environ. Sci. Pollut. Control Ser. 20 (7), 4509–4519.

Dietl, A., Ferousi, C., Maalcke, W.J., Menzel, A., de Vries, S., Keltjens, J.T., Jetten, M.S.M., Kartal, B., Barends, T.R.M., 2015. The inner workings of the hydrazine synthase multiprotein complex. Nature 527 (7578), 394–397.

Gao, D., Huang, X., Tao, Y., 2016. A critical review of NanoSIMS in analysis of microbial metabolic activities at single-cell level. Crit. Rev. Biotechnol. 36 (5), 884–890.

Gao, D.W., Tao, Y., 2011. Versatility and application of anaerobic ammonium-oxidizing bacteria. Appl. Microbiol. Biotechnol. 91 (4), 887–894.

Gori, F., Tringe, S.G., Kartal, B., Marchiori, E., Jetten, M.S., 2011. The metagenomic basis of anammox metabolism in Candidatus 'Brocadia fulgida. Biochem. Soc. Trans. 39 (6), 1799–1804.

Harshman, D.K., Rao, B.M., McLain, J.E., Watts, G.S., Yoon, J.Y., 2015. Innovative qPCR using interfacial effects to enable low threshold cycle detection and inhibition relief. Sci. Adv. 1 (8), e1400061.

Hawley, A.K., Brewer, H.M., Norbeck, A.D., Pasa-Tolic, L., Hallam, S.J., 2014. Metaproteomics reveals differential modes of metabolic coupling among ubiquitous oxygen minimum zone microbes. Proc. Natl. Acad. Sci. U.S.A. 111 (31), 11395–11400.

Hou, X.L., Liu, S.T., Zhang, Z.T., 2015. Role of extracellular polymeric substance in determining the high aggregation ability of anammox sludge. Water Res. 75, 51–62.

Hu, Z.Y., Speth, D.R., Francoijs, K.J., Quan, Z.X., Jetten, M.S.M., 2012. Metagenome analysis of a complex community reveals the metabolic blueprint of anammox bacterium "Candidatus Jettenia asiatica. Front. Microbiol. 3, 366.

Jetten, M.S., Niftrik, L., Strous, M., Kartal, B., Keltjens, J.T., Op den Camp, H.J., 2009. Biochemistry and molecular biology of anammox bacteria. Crit. Rev. Biochem. Mol. Biol. 44 (2–3), 65–84.

Jetten, M.S.M., Strous, M., van de Pas-Schoonen, K.T., Schalk, J., van Dongen, U.G.J.M., van de Graaf, A.A., Logemann, S., Muyzer, G., van Loosdrecht, M.C.M., Kuenen, J.G., 1998. The anaerobic oxidation of ammonium. FEMS Microbiol. Rev. 22 (5), 421–437.

Kartal, B., Kuenen, J.G., van Loosdrecht, M.C., 2010. Sewage treatment with anammox. Science 328 (5979), 702–703.

Kartal, B., Maalcke, W.J., de Almeida, N.M., Cirpus, I., Gloerich, J., Geerts, W., Op den Camp, H.J., Harhangi, H.R., Janssen-Megens, E.M., Francoijs, K.J., Stunnenberg, H.G., Keltjens, J.T., Jetten, M.S., Strous, M., 2011. Molecular mechanism of anaerobic ammonium oxidation. Nature 479 (7371), 127–130.

Kartal, B., Rattray, J., van Niftrik, L.A., van de Vossenberg, J., Schmid, M.C., Webb, R.I., Schouten, S., Fuerst, J.A., Damste, J.S.S., Jetten, M.S.M., Strous, M., 2007. *Candidatus* "Anammoxoglobus propionicus" a new propionate oxidizing species of anaerobic ammonium oxidizing bacteria. Syst. Appl. Microbiol. 30 (1), 39–49.

Kartal, B., Van Niftrik, L., Rattray, J., De Vossenberg, J.L.C.M.V., Schmid, M.C., Damste, J.S., Tetten, M.S.M., Strous, M., 2008. *Candidatus* 'Brocadia fulgida': an autofluorescent anaerobic ammonium oxidizing bacterium. FEMS Microbiol. Ecol. 63 (1), 46–55.

Kopf, S.H., McGlynn, S.E., Green-Saxena, A., Guan, Y.B., Newman, D.K., Orphan, V.J., 2015. Heavy water and ^{15}N labelling with NanoSIMS analysis reveals growth rate-dependent metabolic heterogeneity in chemostats. Environ. Microbiol. 17 (7), 2542–2556.

Kuenen, J.G., 2008. Anammox bacteria: from discovery to application. Nat. Rev. Microbiol. 6 (4), 320–326.

Kuypers, M.M.M., Sliekers, A.O., Lavik, G., Schmid, M., Jorgensen, B.B., Kuenen, J.G., Damste, J.S.S., Strous, M., Jetten, M.S.M., 2003. Anaerobic ammonium oxidation by anammox bacteria in the Black Sea. Nature 422 (6932), 608–611.

Laureni, M., Weissbrodt, D.G., Szivak, I., Robin, O., Nielsen, J.L., Morgenroth, E., Joss, A., 2015. Activity and growth of anammox biomass on aerobically pre-treated municipal wastewater. Water Res. 80, 325–336.

Li, M., Hong, Y.G., Cao, H.L., Gu, J.D., 2011. Mangrove trees affect the community structure and distribution of anammox bacteria at an anthropogenic-polluted mangrove in the Pearl River Delta reflected by 16S rRNA and hydrazine oxidoreductase (HZO) encoding gene analyses. Ecotoxicology 20 (8), 1780–1790.

Li, X.J., Sun, S., Badgley, B.D., Sung, S.W., Zhang, H.S., He, Z., 2016. Nitrogen removal by granular nitritation-anammox in an upflow membrane-aerated biofilm reactor. Water Res. 94, 23–31.

Lin, Y.M., Lotti, T., Sharma, P.K., van Loosdrecht, M.C.M., 2013. Apatite Accumulation Enhances the Mechanical Property of Anammox Granules. Water Research.

Lu, H.F., Zheng, P., Ji, Q.X., Zhang, H.T., Ji, J.Y., Wang, L., Ding, S., Chen, T.T., Zhang, J.Q., Tang, C.J., Chen, J.W., 2012. The structure, density and settlability of anammox granular sludge in high-rate reactors. Bioresour. Technol. 123, 312–317.

Matin, A., 1978. Organic nutrition of chemolithotrophic bacteria. Annu. Rev. Microbiol. 32, 433–468.
Muhammad, A., Mamoru, O., Takanori, A., Kazuo, I., Zenichiro, K., Hiroaki, Y., Daisuke, H., Tomonori, K., Hisashi, S., Takao, F., Satoshi, O., 2015. Physiological characterization of anaerobic ammonium oxidizing bacterium '*Candidatus* Jettenia caeni. Environ. Microbiol. Rep. 17 (6), 2172–2189.
Musat, N., Foster, R., Vagner, T., Adam, B., Kuypers, M.M.M., 2012. Detecting metabolic activities in single cells, with emphasis on nanoSIMS. FEMS Microbiol. Rev. 36 (2), 486–511.
Musat, N., Musat, F., Weber, P.K., Pett-Ridge, J., 2016. Tracking microbial interactions with NanoSIMS. Curr. Opin. Biotechnol. 41, 114–121.
Oshiki, M., Satoh, H., Okabe, S., 2016. Ecology and physiology of anaerobic ammonium oxidizing bacteria. Environ. Microbiol. 18 (9), 2784–2796.
Pitcher, A., Villanueva, L., Hopmans, E.C., Schouten, S., Reichart, G.J., Sinninghe Damste, J.S., 2011. Niche segregation of ammonia-oxidizing archaea and anammox bacteria in the Arabian Sea oxygen minimum zone. ISME J. 5 (12), 1896–1904.
Rother, M., Metcalf, W.W., 2004. Anaerobic growth of Methanosarcina acetivorans C2A on carbon monoxide: an unusual way of life for a methanogenic archaeon. Proc. Natl. Acad. Sci. U.S.A. 101 (48), 16929–16934.
Russ, L., Harhangi, H.R., Schellekens, J., Verdellen, B., Kartal, B., Op den Camp, H.J.M., Jetten, M.S.M., 2012. Genome analysis and heterologous expression of acetate-activating enzymes in the anammox bacterium *Kuenenia stuttgartiensis*. Arch. Microbiol. 194 (11), 943–948.
Schmid, M.C., Hooper, A.B., Klotz, M.G., Woebken, D., Lam, P., Kuypers, M.M.M., Pommerening-Roeser, A., op den Camp, H.J.M., Jetten, M.S.M., 2008. Environmental detection of octahaem cytochrome c hydroxylamine/hydrazine oxidoreductase genes of aerobic and anaerobic ammonium-oxidizing bacteria. Environ. Microbiol. 10 (11), 3140–3149.
Schmid, M.C., Maas, B., Dapena, A., de Pas-Schoonen, K.V., de Vossenberg, J.V., Kartal, B., van Niftrik, L., Schmidt, I., Cirpus, I., Kuenen, J.G., Wagner, M., Damste, J.S.S., Kuypers, M., Revsbech, N.P., Mendez, R., Jetten, M.S.M., Strous, M., 2005. Biomarkers for in situ detection of anaerobic ammonium-oxidizing (anammox) bacteria. Appl. Environ. Microbiol. 71 (4), 1677–1684.
Schouten, S., Strous, M., Kuypers, M.M.M., Rijpstra, W.I.C., Baas, M., Schubert, C.J., Jetten, M.S.M., Damste, J.S.S., 2004. Stable carbon isotopic fractionations associated with inorganic carbon fixation by anaerobic ammonium-oxidizing bacteria. Appl. Environ. Microbiol. 70 (6), 3785–3788.
Strous, M., Fuerst, J.A., Kramer, E.H., Logemann, S., Muyzer, G., Pas-Schoonen, K.T., Van De, Webb, R., Kuenen, J.G., Jetten, M.S., 1999. Missing lithotroph identified as new planctomycete. Nature 400 (6743), 446–449.
Strous, M., Pelletier, E., Mangenot, S., Rattei, T., Lehner, A., Taylor, M.W., Horn, M., Daims, H., Bartol-Mavel, D., Wincker, P., Barbe, V., Fonknechten, N., Vallenet, D., Segurens, B., Schenowitz-Truong, C., Medigue, C., Collingro, A., Snel, B., Dutilh, B.E., Op den Camp, H.J.M., van der Drift, C., Cirpus, I., van de Pas-Schoonen, K.T., Harhangi, H.R., van Niftrik, L., Schmid, M., Keltjens, J., van de Vossenberg, J., Kartal, B., Meier, H., Frishman, D., Huynen, M.A., Mewes, H.W., Weissenbach, J., Jetten, M.S.M., Wagner, M., Le Paslier, D., 2006. Deciphering the evolution and metabolism of an anammox bacterium from a community genome. Nature 440 (7085), 790–794.
van de Graaf, A.A., de Bruijn, P., Robertson, L.A., Jetten, M.S.M., Kuenen, J.G., 1996. Autotrophic growth of anaerobic ammonium-oxidizing micro-organisms in a fluidized bed reactor. Environ. Microbiol. 142 (8), 2187–2196.
van de Vossenberg, J., Woebken, D., Maalcke, W.J., Wessels, H.J.C.T., Dutilh, B.E., Kartal, B., Janssen-Megens, E.M., Roeselers, G., Yan, J., Speth, D., Gloerich, J., Geerts, W., van der Biezen, E., Pluk, W., Francoijs, K.J., Russ, L., Lam, P., Malfatti, S.A., Tringe, S.G., Haaijer, S.C.M., Op den Camp, H.J.M., Stunnenberg, H.G., Amann, R., Kuypers, M.M.M., Jetten, M.S.M., 2013. The metagenome of the marine anammox bacterium '*Candidatus* Scalindua profunda' illustrates the versatility of this globally important nitrogen cycle bacterium. Environ. Microbiol. 15 (5), 1275–1289.
van der Star, W.R., Abma, W.R., Blommers, D., Mulder, J.W., Tokutomi, T., Strous, M., Picioreanu, C., van Loosdrecht, M.C., 2007. Startup of reactors for anoxic ammonium oxidation: experiences from the first full-scale anammox reactor in Rotterdam. Water Res. 41 (18), 4149–4163.
van Niftrik, L., Geerts, W.J.C., van Donselaar, E.G., Humbel, B.M., Yakushevska, A., Verkleij, A.J., Jetten, M.S.M., Strous, M., 2008. Combined structural and chemical analysis of the anammoxosome: a membrane-bounded intracytoplasmic compartment in anammox bacteria. J. Struct. Biol. 161 (3), 401–410.
van Niftrik, L., Jetten, M.S.M., 2012. Anaerobic ammonium-oxidizing bacteria: unique microorganisms with exceptional properties. Microbiol. Mol. Biol. Rev. 76 (3), 585–596.
Walter, J., Melzak, S., Okello, J., Efraime, B., 1999. Key physiology of anaerobic ammonium oxidation. Appl. Environ. Microbiol. 65 (7), 3248–3250.
Ward, B.B., 2013. How nitrogen is lost. Science 341 (6144), 352–353.
Zhu, G.B., Wang, S.Y., Wang, W.D., Wang, Y., Zhou, L.L., Jiang, B., Op den Camp, H.J.M., Risgaard-Petersen, N., Schwark, L., Peng, Y.Z., Hefting, M.M., Jetten, M.S.M., Yin, C.Q., 2013. Hotspots of anaerobic ammonium oxidation at land-freshwater interfaces. Nat. Geosci. 6 (2), 103–107.